Received: 7 February 2024 | Revised: 26 March 2024 | Accepted: 16 April 2024

DOI: 10.1111/liv.15956

Liver INTERNATIONAL WILEY

ORIGINAL ARTICLE

# Thy-1 restricts steatosis and liver fibrosis in steatotic liver disease

Valentin Blank[1,2] | Thomas Karlas[1] | Ulf Anderegg[3] | Johannes Wiegand[4] | Josi Arnold[3] | Linnaeus Bundalian[5] | Gabriela-Diana Le Duc[5,6] | Christiane Körner[7] | Thomas Ebert[8] | Anja Saalbach[3]

[1]Division of Gastroenterology, Department of Medicine II, Leipzig University Medical Center, Leipzig, Germany

[2]Division of Interdisciplinary Ultrasound, Department of Internal Medicine I - Gastroenterology and Pneumology, University Hospital Halle, Halle, Germany

[3]Department of Dermatology, Venereology and Allergology, University of Leipzig Medical Center, Leipzig, Germany

[4]Division of Hepatology, Department of Medicine II, Leipzig University Medical Center, Leipzig, Germany

[5]Institute of Human Genetics, University of Leipzig Medical Center, Leipzig, Germany

[6]Department of Evolutionary Genetics, Max Planck Institute for Evolutionary Anthropology, Leipzig, Germany

[7]Division of Hepatology, Clinic of Oncology, Gastroenterology, Hepatology, and Pneumology, University Hospital Leipzig, Leipzig, Germany

[8]Division of Endocrinology, Department of Medicine III - Endocrinology, Nephrology, Rheumatology, University of Leipzig Medical Center, Leipzig, Germany

**Correspondence**
Anja Saalbach, Department of Dermatology, Venerology and Allergology, University of Leipzig Medical Center, Johannisallee 30, Leipzig 04103, Germany.
Email: anja.saalbach@medizin.uni-leipzig.de

**Funding information**
We acknowledge the support of the University Leipzig within the program Open Access Publishing; ThE was further funded through the EFSD Mentorship Programme supported by AstraZeneca; ThE was supported by a Novo Nordisk postdoctoral fellowship run in partnership with Karolinska Institutet, Stockholm, Sweden; a Karolinska Institute Research Foundation grant; the Stiftelsen Stig och Gunborg Westman; the Swedish Kidney Foundation (Njurfonden); the German Diabetes Association (DDG); and the Team Award Nephrology+ 2023 by Otsuka Pharma; The patient cohorts were recruited from clinical research projects of the IFB AdiposityDiseases Leipzig, Germany (supported by the Federal Ministry of Education and Research [BMBF], Germany; FKZ: 01EO1001);

## Abstract

**Background and Aims:** Steatotic liver disease (SLD) is generally considered to represent a hepatic manifestation of metabolic syndrome and includes a disease spectrum comprising isolated steatosis, metabolic dysfunction-associated steatohepatitis, liver fibrosis and ultimately cirrhosis. A better understanding of the detailed underlying pathogenic mechanisms of this transition is crucial for the design of new and efficient therapeutic interventions. Thymocyte differentiation antigen (Thy-1, also known as CD90) expression on fibroblasts controls central functions relevant to fibrogenesis, including proliferation, apoptosis, cytokine responsiveness, and myofibroblast differentiation.

**Methods:** The impact of Thy-1 on the development of SLD and progression to fibrosis was investigated in high-fat diet (HFD)-induced SLD wild-type and Thy-1-deficient mice. In addition, the serum soluble Thy-1 (sThy-1) concentration was analysed in patients with metabolic dysfunction-associated SLD stratified according to steatosis, inflammation, or liver fibrosis using noninvasive markers.

**Results:** We demonstrated that Thy-1 attenuates the development of fatty liver and the expression of profibrogenic genes in the livers of HFD-induced SLD mice. Mechanistically, Thy-1 directly inhibits the profibrotic activation of nonparenchymal

**Abbreviations:** ECM, extracellular matrix; GPI, glycosylphosphatidylinositol; HFD, high-fat diet; HSCs, hepatic stellate cells; IL, interleukin; IR, insulin resistance; MASH, metabolic dysfunction-associated steatohepatitis; NASLD, metabolically associated steatotic liver disease; SLD, steatotic liver disease; T2D, type 2 diabetes; TG, triglycerides; TGF, transforming growth factor; Thy-1, thymocyte differentiation antigen.

Valentin Blank, Thomas Karlas, Thomas Ebert, and Anja Saalbach contributed equally to this study.

This work was supported by a grant from DFG (SA 863/9-1) and by the DFG SFB 1052 project B10; CK was supported by the BMBF-funded project LiSyM-Cancer [031L0258E; 031L0256C

liver cells. In addition, Thy-1 prevents palmitic acid-mediated amplification of the inflammatory response of myeloid cells, which might indirectly contribute to the pronounced development of liver fibrosis in Thy-1-deficient mice. Serum analysis of patients with metabolically associated steatotic liver disease syndrome revealed that sThy-1 expression is correlated with liver fibrosis status, as assessed by liver stiffness, the Fib4 score, and the NAFLD fibrosis score.

**Conclusion:** Our data strongly suggest that Thy-1 may function as a fibrosis-protective factor in mouse and human SLD.

**KEYWORDS**
metabolic dysfunction-associated, metabolic dysfunction-associated steatohepatitis, steatotic liver disease, steatotic liver disease fibrosis, Thy-1

## 1 | INTRODUCTION

Steatotic liver disease (SLD) includes a disease spectrum ranging from isolated steatosis to metabolically associated steatotic liver disease (MASLD), metabolically associated steatohepatitis (MASH) and ultimately to liver fibrosis and cirrhosis. MASLD is currently considered the most common cause of chronic liver disease.[1–3] Importantly, one-third of patients with MASLD will develop MASH, which contributes to an increased risk of end-stage liver disease, such as liver cirrhosis and hepatocellular carcinoma.[4,5] MASH is the most common cause of cirrhosis in adults awaiting liver transplantation in the United States.[1,5]

Metabolic syndrome, obesity, insulin resistance (IR), type 2 diabetes (T2D), and dyslipidaemia are strongly associated with MASLD. Thus, MASLD can be detected in approximately 75% of obese patients and 70% of overweight patients but also in 25% of normal-weight patients. Approximately, 70% of all patients with T2D develop MASLD.[1,6,7] Due to the global rise in the incidence of these risk factors, the incidence of MASLD is increasing worldwide in the general population and in patients affected by T2D.[6,8]

Pathophysiologically, hepatic steatosis is characterized by triglyceride (TG) accumulation in hepatocytes because of dietary fat intake, de novo lipogenesis, and in some cases, IR. MASH represents a more aggressive manifestation of the disease and is characterized by steatosis, inflammation, hepatocyte cell ballooning and the potential presence of progressive fibrosis.[1,3] When fatty acids overwhelm physiologically adaptive mechanisms in the liver, reactive oxygen species formation, endoplasmic reticulum stress, hepatocellular dysfunction, and cell injury induce inflammation.[9] Macrophages are the most abundant liver immune cells. They play a critical role both in the maintenance of hepatic homeostasis and in liver diseases. Because of their central position in the hepatic microenvironment, long cytoplasmic protrusions, and high expression of pattern recognition receptors, macrophages are the first cells to respond to liver injury. The proliferation of macrophages and the recruitment and differentiation of monocyte-derived macrophages are the cellular sources of liver macrophages.[10] Persistent inflammation in turn drives fibrosis, ultimately leading to liver cirrhosis. The hallmark of hepatic fibrosis is the increased expression and deposition of extracellular matrix (ECM), which progressively destroys liver architecture and function. ECM-producing cells can originate from many sources, including hepatic stellate cells (HSCs), portal myofibroblasts, resident fibrocytes, vascular smooth muscle cells, and hepatocytes, upon activation or transdifferentiation.[11] Macrophages interact with all of these cells through soluble mediators that control viability, proliferation, and activation. Thus, hepatic macrophages are the main players in the pathogenesis of liver fibrosis.[10]

**Key points**

Steatotic liver disease (SLD) and its disease spectrum comprising of isolated steatosis, steatohepatitis, liver fibrosis and ultimately cirrhosis contributes to increased morbidity and mortality of affected individuals. Therefore, potential treatment candidates need to be developed to reduce the burden of this disease. Thymocyte differentiation antigen (Thy-1, CD90) expression on fibroblasts controls central functions relevant to fibrosis. Our data strongly suggest that Thy-1 may function as a fibrosis-protective factor in SLD. Genetic mouse models, detailed in vitro studies, and studies on human patients with SLD indicate that Thy-1 appears to be an attractive treatment candidate for SLD.

Dynamic molecular network and coexpression analyses revealed nine genes (*COL3A1*, *CXCL9*, *CYCS*, *CXCL10*, thymocyte differentiation antigen [*THY-1*], *COL1A2*, *SAA1*, *CDKN1A*, and *JUN*) that were associated with healthy-to-SLD, obesity-to-SLD, and progression. All the genes were positively correlated with the NAFLD activity score. *CDKN1A* correlated with age, *CYCS* with lobular inflammation and cytological ballooning grade, and *CXCL10* with steatosis grade. Importantly, THY-1 was the most relevant gene correlated with fibrosis stage.[12]

Thy-1 is a highly glycosylated, glycosylphosphatidylinositol (GPI)-anchored membrane protein.[13] Its expression is restricted to fibroblasts, neurons, activated microvascular endothelial cells, glomerular cells, a subpopulation of haematopoietic stem cells, and

mesenchymal stem cells. In mice, Thy-1 is also expressed in T cells.[13] Thy-1 can also be cleaved from the cell surface by phospholipase C or D.[14] Soluble Thy-1 (sThy-1) can be detected in biological fluids such as serum, wound fluid from venous leg ulcers, and synovial fluid from joints in rheumatoid arthritis.[15] The effect of Thy-1 on fibroblasts controls central functions relevant to fibrogenesis, including proliferation, apoptosis, cytokine and growth factor expression and responsiveness, cell adhesion, migration, ECM deposition, and myofibroblast differentiation.[16] Consistent with these findings, mice lacking *Thy-1* develop more severe fibrosis, including bleomycin-induced lung fibrosis, an experimental model of cardiac hypertrophy and heart failure, *Mdr2* deficiency-induced liver fibrosis, and unilateral urinary obstruction-induced kidney fibrosis, than wild-type controls do.[17–19] Tissue analysis indicated that *Thy-1* deficiency is associated with increased expression of profibrotic genes, such as collagen types I and III, alpha smooth muscle cell actin, and transforming growth factor beta (TGFβ) receptor I. Loss of THY-1 expression in activated fibroblasts within fibroblastic foci in human idiopathic pulmonary fibrosis proves its relevance for human disease.[20] However, in contrast to pulmonary, renal, and liver tissue data, *Thy-1*-deficient mice develop attenuated skin fibrosis in both bleomycin and tight skin-1 mouse models and exhibit impaired myofibroblast differentiation and ECM deposition during skin wound healing, suggesting that Thy-1 plays a tissue-specific role in organ fibrosis.[21,22] Dudas et al. showed that Thy-1 is a functional marker of liver myofibroblasts in normal, injured, and regenerating rat livers.[23]

Taken together, these findings suggest that Thy-1 is directly involved in fibrosis development in different organs. However, because of the tissue-specific effects of Thy-1, it remains unclear whether increased Thy-1 expression is functional for the development of liver fibrosis or represents a regulatory mechanism counteracting the fibrotic reaction. Therefore, we investigated the role of Thy-1 in the development of fatty liver and subsequent fibrosis in a mouse model of high-fat diet (HFD)-induced SLD. Finally, we demonstrated the relevance of Thy-1 for SLD progression by detecting circulating Thy-1 in patients with MASLD.

## 2 | METHODS

### 2.1 | Human studies

We recruited two different cohorts comprising patients with SLD. At the time of recruitment, patients were classified by the former NAFLD criteria and nomenclature.[24] According to the Delphi consensus statement, we used the novel MASLD term for reporting patient data in our SLD cohorts.[25]

#### 2.1.1 | Patient cohort I

First, the serum Thy-1 concentration was analysed in healthy probands ($n=15$) and patients ($n=94$) with established MASLD diagnoses from two previously described cohorts.[26,27] The initial purpose of these studies was to characterize the diagnostic performance of vibration controlled transient elastography (VCTE) and controlled attenuation parameter (CAP) in patients with MASLD. Details on recruitment, patient characterization, and sample processing are described in detail here.[26,27] The studies were approved by the local ethical committee (Leipzig University, registration numbers 283-11-22082011 and 419-12-17122012). Informed written consent was obtained from all participants, and the studies were performed in accordance with the guidelines for good clinical practice and the ethical guidelines of the Helsinki Declaration.

#### 2.1.2 | Patient cohort II – T2D patients

Since MASLD is a major health burden for patients with T2D, we investigated a second cohort of exclusively T2D patients ($n=180$). These patients were prospectively investigated to evaluate the performance of established NAFLD guidelines for risk stratification of hepatic fibrosis.[28] The study was approved by the local ethical committee (Leipzig University, registration number 035/17-ek) and registered in the German Clinical Trials Register (DRKS00012281). Informed written consent was obtained from all participants, and the study was performed in accordance with the guidelines for good clinical practice (E6/R1) and the ethical guidelines of the Helsinki Declaration.

### 2.2 | Liver elastography and estimation of hepatic steatosis

VCTE allows noninvasive estimation of hepatic fibrosis and steatosis. Elastography measurements (FibroScan; Echosens, Paris, France) were performed using the appropriate probe (M or XL-probe, 3.5/2.5 MHz, respectively), defined by the skin-to-liver-capsule distance (M-probe ≤25 mm; XL-probe >25 mm). VCTE was performed by a trained certified examiner in accordance with established guidelines as described previously.[3,28,29] Elevated liver stiffness measurements (LSM) indicated suspicion of significant liver fibrosis. A liver stiffness value of ≥12 kPa was used to define the risk of significant fibrosis, and a value <8 kPa was used to rule out relevant fibrosis. In addition to the LSM, the VCTE device calculates the CAP as a surrogate for the severity of hepatic steatosis, expressed in dB/m.[30] The steatosis grade was estimated according to the CAP value using previously defined cut-off values for patients at risk for SLD. A CAP above 331 dB/m was considered to indicate a high risk of advanced steatosis.

### 2.3 | FAST score

To identify patients with active MASH (activity score ≥4) and significant fibrosis ($F\geq 2$), an elastography-based scoring system (FAST

score) using VCTE was recently established.[30,31] The score was calculated from the LSM, CAP, and AST (described in detail in[32]). At a cut-off of .35, the score achieved a sensitivity of ≥.90 for the diagnosis of MASH, and a cut-off of .67 had a specificity of ≥.90.[30] In this study, the FAST score was used to assess the risk of hepatic inflammation.

## 2.4 | Laboratory-based fibrosis risk scores

Nonalcoholic fatty liver disease fibrosis score (NFS):

$$\begin{aligned}\text{NFS} &= -1.675 + 0.037 \times \text{age [years]} + 0.094 \times \text{BMI}\left[\text{kg/m}^2\right] + (1.13 \times \text{diabetes}\ [\text{yes} = 1, \text{no} = 0]) \\ &\quad + (0.99 \times \text{AST/ALT ratio}) - (0.013 \times \text{platelet}\ [\text{Gpt/L}]) \\ &\quad - (0.66 \times \text{albumin}\ [\text{g/dL}]).\end{aligned}$$

The sensitivity and specificity cut-off values used were −1.455 (age 36–65) and .12 (age ≥ 65) and .676 (age ≥ 36), respectively.[30]
FIB-4 score:

$$\text{FIB} - 4 = (\text{age [years]} \times \text{AST}\ [\text{U/L}]) / (\text{platelet}\ [\text{Gpt/l}] \times (\text{ALT}\ [\text{U/L}])1/2).$$

The sensitivity and specificity cut-off values used were 1.3 (age < 65) and 2.0 (age ≥ 65) and 2.67 (all ages), respectively.[33,34]

## 2.5 | Detection of human sThy-1

High-binding ELISA plates (Sarstedt, Nürnbrecht, Germany) were coated with .25 μg/well anti-THY-1 antibody (clone AS02; Dianova, Hamburg, Germany) in .1 M $NaHPO_4$/.1 M $NaH_2PO_4$, pH 9.0, overnight at 4°C. After three washes with PBS/.05% Tween 20, the plates were blocked with PBS/10% foetal calf serum (FCS) for 1 h at 4°C. After several washes with PBS/.05% Tween 20, the samples and standard (recombinant Thy-1-Fc; R&D, Minneapolis, USA; 5000 pg/mL–7.8 pg/mL) were diluted in PBS/10% FCS and incubated overnight at 4°C. After five washes with PBS/.05% Tween 20. Then, .5 μg/mL biotinylated anti-CD90 monoclonal antibody (clone 5E10; Pharmingen, Hamburg, Germany) was added for 90 min at room temperature. Next, the washing procedure was repeated, and avidin-conjugated peroxidase (Invitrogen) diluted 1:500 in PBS/10% FCS was added for 1 h at room temperature. The plates were rinsed five times with PBS/.05% Tween 20. Finally, tetramethylbenzidine was added, after which the reaction was stopped by 10 min with 1 M $H_2SO_4$, after which the absorbance of the samples was measured at 405 nm.

## 2.6 | Animal studies

Thy-1 deficient (KO) mice were kindly provided as a gift from Dr. R. Morris (King's College London, UK,[35]). *Wt/db* and *db/db* female mice were obtained from Janvier laboratories (Le Genest-Saint-Isle, France). Mice were sacrificed at 12–14 weeks of age. Mice were kept under a 12-h light–dark cycle and given food and water ad libitum.

Four-week-old male Thy-1 KO mice and WT C57BL/6J mice were fed either a HFD containing 35.7% fat (59% of calories from fat; EF R/M D12331 diet modified by Surwit, ssniff) or a control (chow) diet for 18 weeks.

All animal experiments were performed in accordance with institutional and state guidelines and approved by the Committee on Animal Welfare of Saxony (TVV03/16, TVV13/19, T05/20).

## 2.7 | RNA sequencing analysis of mouse liver

RNA from the livers of three wild-type and three Thy-1-KO mice was prepared using the ReliaPrep RNA Miniprep system (Promega, Walldorf, Germany) according to the manufacturer's protocol. The RNA integrity and concentration were examined on an Agilent Fragment Analyzer (Agilent Technologies, Palo Alto, CA, USA) using an HS RNA Kit (Agilent) according to the manufacturer's instructions.

Sequencing was performed according to Kaiser et al.[36] Briefly, 100 ng of total RNA was depleted of ribosomal RNA using the NEBNext® rRNA Depletion Kit v2 (NEB, Frankfurt a.M., Germany) according to the manufacturer's instructions. The depleted RNA was transcribed using SuperScript IV reverse transcriptase (Thermo Fisher, Waltham, MA, USA) for 2 h at 55°C. After second strand synthesis (TargetAmp Kit [Epicentre]), the DNA was tagmented using the Illumina Tagment DNA TDE1 Enzyme and Buffer Kits, which fragment the DNA and insert partial sequencing adapter (Nextera) sequences. Final PCR amplification of the libraries was performed using a KAPA HiFi HotStart Library Amplification Kit with unique dual indexing by IDT® for Illumina Nextera DNA Unique Dual Indices Sets. The barcoded libraries were purified and quantified using Qubit Fluorometric Quantification (Thermo Fisher Scientific). The size distribution of the library DNA was analysed using a FragmentAnalyzer (Agilent). Sequencing of 2 × 150 bp was performed with a NovaSeq sequencer (Illumina, San Diego, CA, USA) according to the manufacturer's instructions. After demultiplexing with bcl2fastq software (Illumina, v2.20) and polishing using fastp,[37] only sequences longer than 20 bp were further analysed. Reads were mapped against the mouse reference genome (GRCm39) using HISAT2.[38] Stringtie and the R package Ballgown[39] were used to calculate the differential expression. The expression data were normalized using the DESeq2[40] R bioconductor package.

For the data analysis, 53 598 genes were identified. The mean signal strengths of the WT and Thy-1-KO mice were calculated, and the *p* value (Student's *t*-test) and x-fold change were calculated. Genes with a change between .5 and 2-fold and a *p* value < .05 were subjected to functional class analysis via overrepresentation analysis (ORA) implemented in the R package *clusterProfiler*.[41] The method uses a hypergeometric test[42] to assess the probability of observing at least *k* genes from the list across the pathway database, which can be expressed as follows:

$$P(X \geq k \mid n; N; K) = \sum_{i=k}^{n} \frac{\binom{K}{i}\binom{N-K}{n-i}}{\binom{N}{n}}.$$

The database used in the analysis was the Gene Ontology (GO) biological process database.[43,44] Genes with a change between .5 and 2-fold and a $p$ value < .05 (677 genes) were log2-transformed and plotted in the heatmap using R with the *tidyverse* and *reshape* package.[45,46]

## 2.8 | Gene expression analysis (RT–qPCR)

Total RNA was isolated from the mouse tissue and cells using the ReliaPrep RNA Miniprep system (Promega) according to the manufacturer's protocol. Total RNA (.5 μg) was used for cDNA synthesis using LunaScript RT Supermix (New England Biolabs, Ipswich, MA, USA) according to the manufacturer's instructions. Real-time qPCR was performed with LunaUniversal qPCR Mastermix (New England Biolabs) following the manufacturer's instructions. Quantitative gene expression was calculated from the standard curve of the cloned cDNA and normalized to the reference gene RPL36. The sequences of primers used are listed in Table S1.

## 2.9 | Cell isolation/culture

*NPC: Liver* tissue was digested using the Liver Dissociation Kit from Miltenyi (Bergisch-Gladbach, Germany) according to the manufacturer's protocol. The cells were filtered through a 70 μm filter and washed several times. The cells were cultured in DMEM supplemented with 10% FCS (Pan-Biotech), 1% penicillin/streptomycin (Biochrom, Berlin, Germany), and insulin–transferrin–selenium-supplemented medium (1:1000, Gibco). The cells were detached using TrypLE Express (Gibco, Waltham, MA, USA).

*$CD11b^+$ cells* were isolated from the liver by magnetic cell separation using CD11b beads (Miltenyi, Bergisch-Gladbach, Germany) according to the manufacturer's protocol.

*Bone marrow cells* were obtained by flushing the leg bones with RPMI (Anprotec, Bruckberg, Germany). The cell suspension was filtered through a 70 μm filter, and erythrocytes were lysed (155 mM NH4CL, 10 mM KHCO3, 1 mM EDTA, pH 7.4) for 2 min. The remaining bone marrow cells were plated at 37°C and 5% $CO_2$ in RPMI (Anprotec, Bruckberg, Germany) supplemented with 10% foetal calf serum (FCS; PAN-Biotech, Aidenbach, Germany), 1% penicillin/streptomycin (Biochrom, Berlin, Germany) and 5 ng/mL M-CSF (Miltenyi, Bergisch-Gladbach, Germany).

For culture of bone marrow cells (BMC) on recombinant mouse Thy-1 (rThy-1), 96-well Sartorius high-binding plates (Sartorius, Göttingen, Germany) were coated with 4 μg/mL rThy-1 fused to the Fc-protein (Invitrogen) or as a control with the Fc-protein (Invitrogen) in coating buffer containing .2 M $Na_2CO_3$ and .2 M $NaHCO_3$ (pH 9.5) overnight at 4°C. After several washes, the plates were blocked with DMEM containing 10% FCS for 30 min. BMC were cultured on coated plates for 4 h. Then, LPS (100 ng/mL; Sigma–Aldrich) and 500 μM PA-BSA complex or BSA alone were added. PA-BSA complexes were prepared as described by Stelzner et al.[47]

## 2.10 | Functional assays

*Cell growth* analysis was performed after 3 days of culture by a 2,3-bis-(2-methoxy-4-nitro-5-sulfophenyl)-2H-tetrazolium-5-carboxanilide salt (XTT) assay (Roche, Mannheim, Germany). The absorbance at 490 nm was measured 2 h after the addition of XTT using a microplate reader (BioTek Instruments).

The activity of *caspase 3/7* was measured using a Caspase-Glo® 3/7 Assay (Promega, Madison, USA) according to the manufacturer's protocol. The luminescence signal was detected after 3 days using a microplate reader (BioTek Instruments).

## 2.11 | ELISA

Murine TNFa, interleukin (IL-1b), and IL-6 were detected via ELISA according to the manufacturer's instructions (Invitrogen, Massachusetts, USA). Insulin was detected by ELISA (Mercodia, Uppsala, Sweden). Serum triglycerides (TG) were analysed by the Triglyceride Assay Kit (Abcam, Berlin, Germany).

## 2.12 | Tissue staining

Frozen liver sections were incubated overnight with mouse anti-CD11b-PE (Miltenyi), and washing was performed using PBS/.05% Tween 20. Nuclei were stained with DAPI. Sections were analysed and photographed using a fluorescence microscope BZ-X810 (Keyence, Neu-Isenburg, Germany) and BZ-X800 Viewer software. The oil-red positive area/microscopic field was calculated using the BZ-X800 Viewer software. Positive stained cells per microscopic field were counted using the BZ-X800 Viewer software.

Triglyceride accumulation was monitored by Oil Red O staining. Tissue sections were fixed in 60% buffered acetone for 15 min at RT, washed with PBS and stained with Oil Red O solution (Sigma). Unbound dye was removed by thorough rinsing with water, and the cells were photographed with a BZ-9000Z microscope (Keyence, Neu-Isenburg, Germany).

## 2.13 | FACS

The phenotype of the isolated cells was determined by flow cytometry using the following antibodies: anti-CD11b and anti-CD90 (Miltenyi, Bergisch-Gladbach, Germany). Flow cytometry was performed using BD FACSLyric flow cytometers (BD Bioscience, Franklin Lakes, New Jersey, U.S.), and the data were analysed using the software BD FACSuite RUOv1.3 (BD Bioscience, Franklin Lakes, New Jersey, U.S.).

### 2.14 | Statistical analyses

IBM SPSS Statistics software version 28.0 (IBM, Armonk, NY) was used for correlation analyses. The nonparametric Spearman's rank correlation method was used to assess univariate relationships between sThy1 and the indicated markers. Multivariate regression analysis was performed for sThy1 (dependent variable) adjusted for sex, age, BMI, and diabetes status. Nonnormally distributed variables were assessed by the Shapiro–Wilk test and logarithmically transformed prior to multivariate testing (Lg). GraphPad Prism 9 (GraphPad Software, San Diego, CA) was used for significance analysis between two or more groups. Normality was tested by the D'Agostino and Pearson normality test or Shapiro–Wilk test ($n \leq 4$). Normally distributed data were analysed using two-tailed Student's *t*-tests; when normality was absent, the Mann–Whitney test was used. For statistical comparisons of more than two groups, one-way ANOVA was used. *p* Values of .05 or less were considered to indicate statistical significance. The different degrees of significance are indicated as follows: $^{*}p < .05$; $^{**}p < .01$; $^{***}p < .001$; and $^{****}p < .0001$.

## 3 | RESULTS

### 3.1 | Thy-1 deficiency aggravates steatosis and liver fibrosis in HFD-induced SLD

HFD induced strong fat accumulation in the liver, as detected by Oil Red O staining (Figure S1A). Elevated hepatic mRNA expression of collagen I (α1), collagen III (α1), and *Tgfβ1* indicates the initiation of a fibrotic response in HFD-fed mice compared with controls (Figure S1B). *Thy-1* gene expression in the liver was not affected by HFD (Figure S1B). In contrast, the serum sThy-1 concentration was significantly increased in obese mice (Figure S1C). Similarly, compared with healthy wt/db mice, C57BLKS/J *db/db* mice, another model of SLD-associated liver fibrosis, exhibited significantly increased mRNA expression of collagen I (α1), collagen III (α1), and *Tgfβ1* in the liver (Figure S1D). However, hepatic *Thy-1* mRNA expression was not affected (Figure S1D), while the serum sThy-1 concentration was significantly greater in *db/db* mice than in control mice (Figure S1E).

To investigate the impact of Thy-1 on the pathogenesis of HFD-induced SLD, wild-type and whole-body Thy-1-knockout mice (Thy-1-KO) were fed a HFD for 18 weeks. A lack of *Thy-1* resulted in increased blood triglyceride and insulin concentrations upon HFD (Figure 1A,B). Consistently, the loss of *Thy-1* exacerbated hepatic fat accumulation in the liver, as detected by Oil Red O staining (Figure 1C). Quantification of fat accumulation via detection of Oil Red O-positive areas (Figure 1D) confirmed pronounced steatosis in Thy-1-KO mice. A strong increase in peroxisome proliferator-activated receptor g (*Pparγ*) mRNA expression confirmed the initiation of an adipogenic gene expression program and the storage of lipids in the livers of Thy-1-KO mice (Figure 1E). RNA sequencing data revealed a significant impact of *Thy-1* knockout on gene expression in the liver, as demonstrated by the clear discrimination of the two genotypes in the heatmap of the differentially expressed genes (DEGs) (Figure 2A). A total of 677 genes were differentially expressed and exhibited at least two-fold changes (458 upregulated, 219 downregulated) in Thy-1-KO mice compared with control mice (Table S1). Consistent with the increase

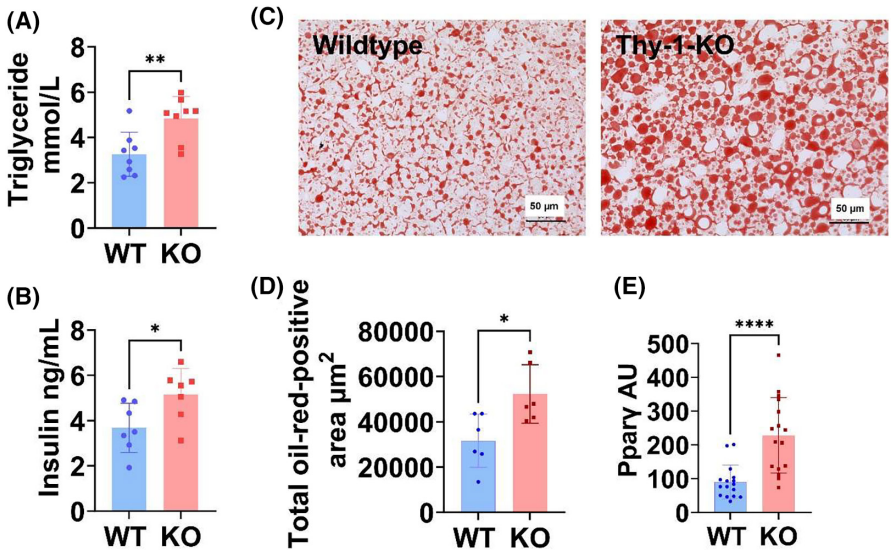


FIGURE 1 Thy-1 deficiency exacerbates hepatic steatosis development during high-fat diet consumption. Wild-type (WT) and whole-body Thy-1 knockout (KO) mice were fed a high-fat diet (HFD) for 18 weeks. (A–B) Detection of serum triglycerides and insulin. (C) Oil Red O staining of liver sections from wild-type and Thy-1-KO mice. One example of five different mice per genotype is shown (bar = 50 µm). (D) Quantification of Oil Red O staining as the total area of Oil Red O-positive cells/microscopic field. (E) Expression of *Pparg* in the liver detected by quantitative PCR. Each point represents one mouse. The results are shown as the mean ± standard deviation. *p* Values were assessed by unpaired Student's *t*-tests. $^{*}p < .05$; $^{**}p < .01$; $^{****}p < .0001$.

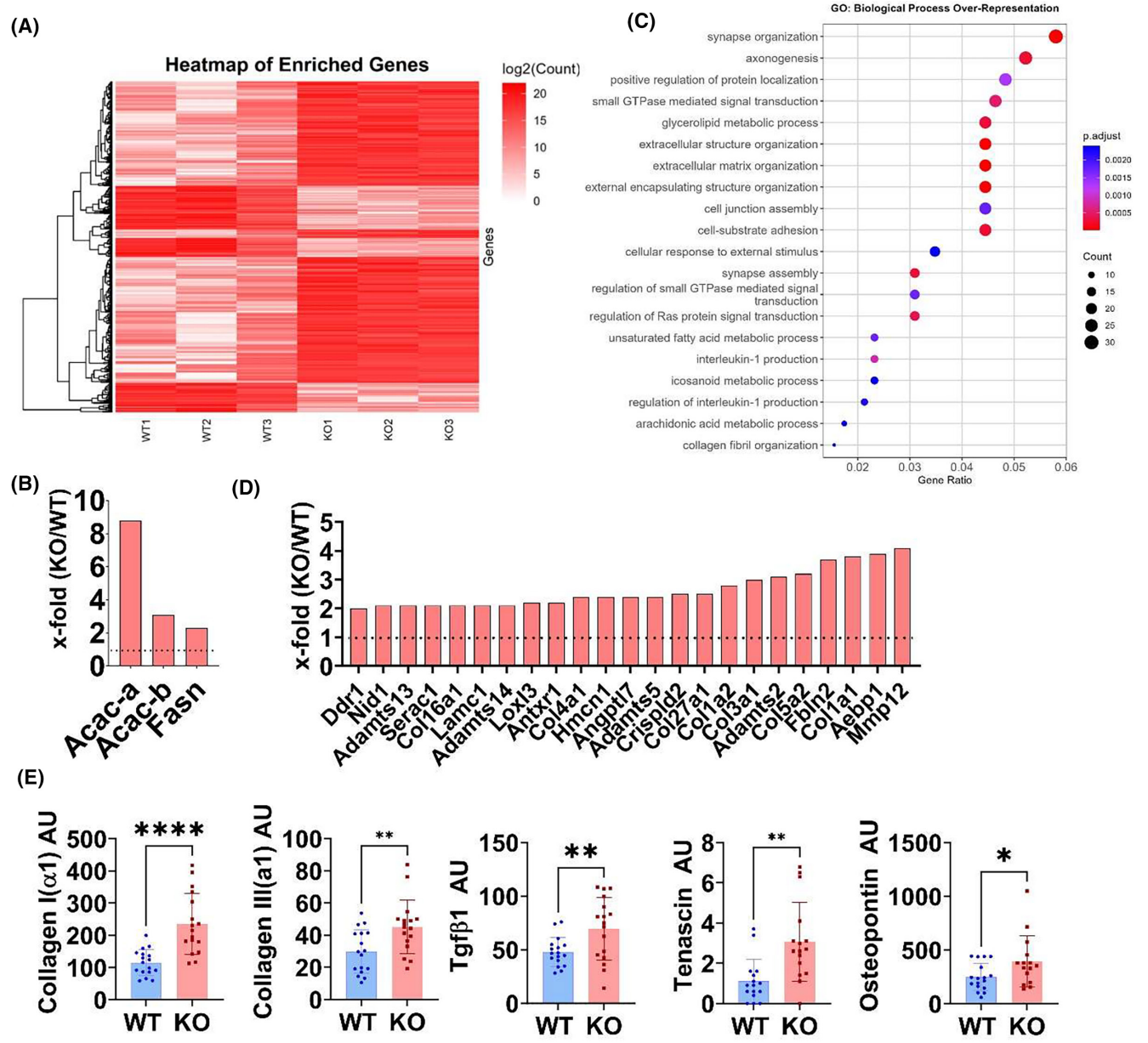


**FIGURE 2** Thy-1 deficiency induces a profibrotic response in HFD-induced SLD mice. Wild-type (WT) and whole-body Thy-1 knockout (KO) mice were fed a high-fat diet (HFD) for 18 weeks. (A) Bulk mRNA sequencing analysis of liver tissue from wild-type and Thy-1-KO mice after 18 weeks of HFD feeding. The DEGs (with a .5-fold change and a two-fold change and a $p$ value < .05) were log2-transformed and subjected to heatmap analysis; (B) Fold change (Thy-1-KO/WT) in genes related to lipogenesis. (C) Genes with a two-fold change and a $p$ value < .05 were subjected to functional class analysis via overrepresentation analysis. (D) Fold change (Thy-1-KO/WT) in genes related to matrix organization identified via functional class analysis. (E) Gene expression of the indicated genes determined by quantitative PCR. Each point represents one mouse. The results are shown as the mean ± standard deviation. $p$ Values were assessed by unpaired Student's $t$-tests. $^{*}p < .05$; $^{**}p < .01$; $^{****}p < .0001$.

in steatosis in Thy-1-KO mice, the expression of genes involved in lipogenesis, such as acetyl-CoA carboxylase (*Acc-A* [*Acac-a*] and *Acc-B* [*Acac-b*]), and fatty acid synthase (*Fasn*), was strongly increased in Thy-1-KO mice (Table S1, Figure 2B). GO pathway analysis demonstrated that Thy-1 regulated different metabolic processes (Figure 2C). After underpinning our hypothesis that Thy-1 is a negative regulator of fibrosis, GO pathway analysis indicated that Thy-1 deletion resulted in the enrichment of genes related to ECM biosynthesis (Figure 2C,D). As shown in Figure 2D, matrix organizing genes, including different collagens and glycoproteins, were expressed at higher levels in Thy-1-KO mice than in wild-type (WT) mice. To underline the RNA sequencing data, quantitative PCR was performed on a separate set of animals. Indeed, the expression of ECM-related genes, such as collagen I (α1), collagen III (α1), tenascin, osteopontin, and *Tgfβ1*, was significantly elevated in the livers of HFD-fed Thy-1-KO mice compared with those of wild-type mice (Figure 2E).

### 3.2 | Thy-1 directly inhibits the activation of nonparenchymal liver cells (NPCs)

The heterogeneous group of nonparenchymal cells includes mainly liver sinusoidal endothelial cells, macrophages, and dendritic cells. The minor fraction of liver NPCs is composed mainly of innate immune cells, comprising natural killer (NK) cells, NKT cells, biliary epithelial cells, and HSCs. Moreover, NPC plays an important role in immune regulation.[48] To obtain insights into the mechanisms of Thy-1-mediated inhibition of liver fibrosis, NPCs were isolated from the livers of HFD-fed wild-type and Thy-1-KO mice. After cell culture, the NPC fraction contained mainly $CD11b^+$ myeloid cells and fibroblasts ($CD90^+$, Figure S2A). Contamination with hepatocytes was excluded by quantifying the expression of albumin, which was almost undetectable in the NPC fraction (Figure S2B). As shown in Figure 3A, NPC cells from Thy-1-KO mice expressed significantly more Ki67, a marker of proliferating cells. Moreover, loss of Thy-1 resulted in increased expression of fibrosis-associated genes, such as collagen I (α1), III (α1) and *Plod2* (Figure 3B). To determine the impact of Thy-1 on the profibrotic action of NPCs, NPCs were isolated from wild-type mice and cultured on recombinant Thy-1-Fc-protein. Fc-protein was used as a control. Consistent with these findings, culture of NPC cells with recombinant Thy-1 strongly reduced proliferation compared with culture with the Fc-control protein, as detected by XTT and microscopy (Figure 3C,D). The detection of active caspase-3/7 demonstrated that apoptosis was stimulated by Thy-1 compared with the control protein (Figure 3E). Consistent with these findings, the increased expression of profibrotic genes, such as collagen I (α1), collagen III (α1) and *Plod2*, in NPC from Thy1-KO mice (Figure 3B) and recombinant Thy-Fc-protein inhibited the expression of these genes in NPCs (Figure 3F). Taken together, these findings suggest that Thy-1 inhibits the profibrotic activation of NPCs.

### 3.3 | Thy-1 restricts the proinflammatory activation of myeloid cells

The interaction of hepatic macrophages with other cell types in the liver, including HSCs, endothelial cells, neutrophils, and platelets, contributes to the pathogenesis of various liver diseases, such as the development of liver fibrosis. Therefore, the impact of Thy-1 expression on the activation of myeloid cells was analysed. First, the number of inflammatory cells within the livers of HFD-fed WT- and Thy-1-KO mice was analysed via immunofluorescence staining of $CD11b^+$ cells. As shown in Figure 4A,B, loss of Thy-1 resulted in a significantly increased infiltration of $CD11b^+$ cells. Next, $CD11b^+$ myeloid cells were isolated from the livers of HFD-fed WT- and Thy-1-KO mice. Interestingly, loss of Thy-1 resulted in increased activation of myeloid cells, as demonstrated by increased expression of proinflammatory cytokines, such as IL-1b and TNFa, as well as Ki67, a marker of proliferating cells (Figure 4C). In contrast, typical markers of M2-like macrophages were not affected by Thy-1 (Figure S3).

To understand the action of Thy-1, bone marrow cells were isolated from WT mice and cultured on recombinant Thy-1-Fc or Fc-protein. To imitate the proinflammatory environment in SLD, cells were stimulated with lipopolysaccharide (LPS) and 500 μM palmitic acid (PA)/bovine serum albumin complex (BSA). Cells without LPS or PA/BSA were used as controls. LPS induces the secretion of IL-1β, IL-6, and TNFα from BMC, while PA amplifies this LPS response. Most importantly, Thy-1 prevents the PA-mediated amplification of the secretion of these inflammatory cytokines (Figure 5A). RNA analysis revealed that Thy-1 inhibits the PA-mediated amplification of the gene expression of proinflammatory cytokines, chemokines and Toll-like receptor 4 (Tlr4) but does not affect the LPS response itself (Figure 5B).

### 3.4 | Serum sThy-1 levels positively correlate with liver fibrosis in patients with MASLD

To prove the important role of Thy-1 in the development of a fibrotic response during SLD in human patients, serum sThy-1 was analysed in two independent cohorts comprising patients with MASLD in parallel to parameters of hepatic fibrosis risk (i.e., liver stiffness, NAFLD fibrosis score and Fib4 score), fibrotic inflammation (FAST score), and steatosis severity (CAP). The clinical characteristics of both MASLD study populations are shown in Table 1. Furthermore, sThy-1 was also detected in the serum of healthy subjects ($n = 15$; 9 females, 6 males; mean age = 38.5 ± 16.5 years [21]). Patients were stratified according to their risk of steatosis, inflammation, and fibrosis grade. Cohort 1 ($n = 94$) included diabetic and nondiabetic patients. As shown in Figure 6, hepatic steatosis, as assessed by the CAP, did not affect the serum sThy-1 concentration in this cohort. There was a slight but not statistically significant increase in the risk of steatohepatitis characterized by the FAST score (Figure 6). Importantly, sThy-1 expression increased significantly with increasing fibrosis risk, as characterized by liver stiffness determined by elastography (VCTE), the NAFLD fibrosis score, and the Fib4 score in cohort 1 (Figure 6).

Since MASLD is frequently observed in patients with T2D, we analysed sThy-1 in a second cohort of exclusively T2D patients ($n = 180$). However, the circulating sThy-1 concentration did not depend on steatosis severity (Figure 6; Table 2). Furthermore, we observed a significant increase in sThy-1 expression with increasing risk of steatohepatitis (FAST score; Figure 6) in this larger cohort of patients specifically selected for T2D. Finally, we demonstrated the relationship between increased sThy-1 serum levels and a higher risk of advanced fibrosis, for example, NAFLD fibrosis score (Figure 6).

To determine the associations of sThy-1 with steatosis grade, steatohepatitis status, and fibrosis risk, we performed univariate correlations and multivariate linear regression analyses separately for each of the cohorts. According to the univariate correlation analysis, the serum levels of sThy-1 in the first cohort were significantly and positively correlated with the AST, NAFLD fibrosis score, Fib4 score, liver stiffness, and FAST score (Table 2). CAP showed a weak

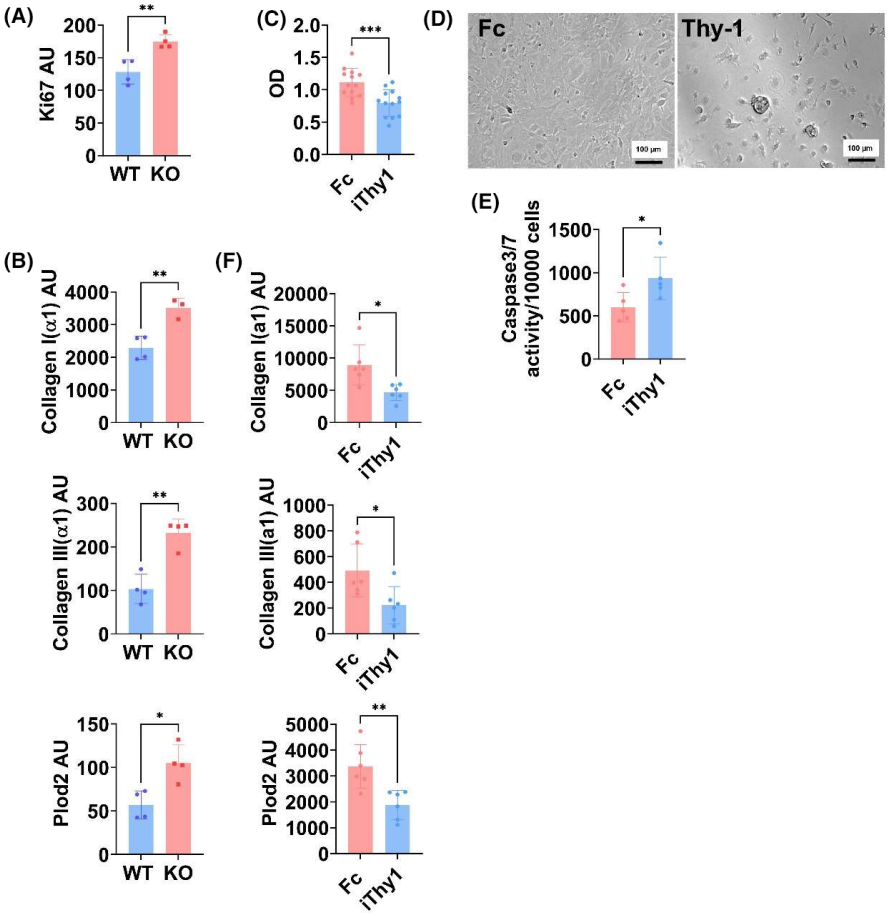


**FIGURE 3** Thy-1 directly inhibits the activation of nonparenchymal liver cells (NPC). (A, B) NPCs were isolated from the livers of HFD-fed WT- and Thy-1-KO mice. The expression of the indicated genes was analysed by quantitative PCR. (C–E) NPC were isolated from WT mice and cultured with recombinant Thy-1-Fc-protein (iThy1) or control protein (Fc). (C) Cell growth was detected after 3 days of treatment with XXT. (D) Microscopy images of NPC cultured on Thy-1 and Fc-control proteins after 3 days. One representative example of 5 different experiments is shown. (E) Apoptosis was determined by a caspase 3/7 activation assay after 3 days. (F) Gene expression of the indicated genes was detected by quantitative PCR after 24 h. Each point represents one mouse. The results are shown as the mean ± standard deviation. *p* Values were assessed by unpaired Student's *t*-tests. $^{*}p < .05$; $^{**}p < .01$; $^{***}p < .001$p.

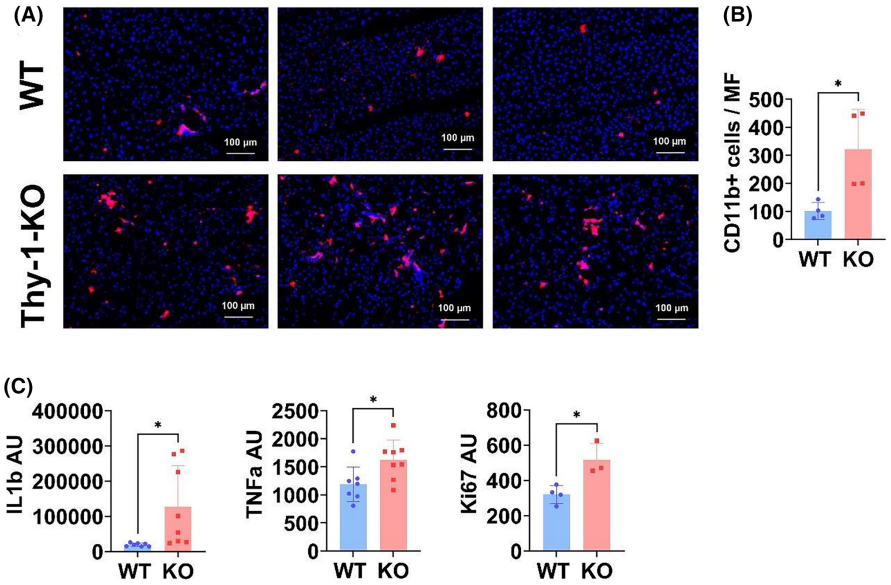


**FIGURE 4** Thy-1 restricts the infiltration and activation of inflammatory cells during the development of fatty liver in HFD-induced SLD mice. Wild-type (WT) and whole-body Thy-1 knockout (KO) mice were fed a high-fat diet (HFD) for 18 weeks. (A) Inflammatory cells in the liver were stained with an anti-CD11b antibody (red). Nuclei were counterstained with DAPI (blue). Images of three different WT and Thy-1-KO are shown. (B) $CD11b^{+}$ cells were counted per microscopic field using Keyence software. Each dot represents the number of positive cells/microscopic fields per animal. (C) $CD11b^{+}$ cells were isolated from the liver by magnetic cell separation. The expression of the indicated genes was detected by quantitative PCR. Each point represents one mouse. The results are shown as the mean ± standard deviation. *p* Values were assessed by unpaired Student's *t*-tests. $^{*}p < .05$.

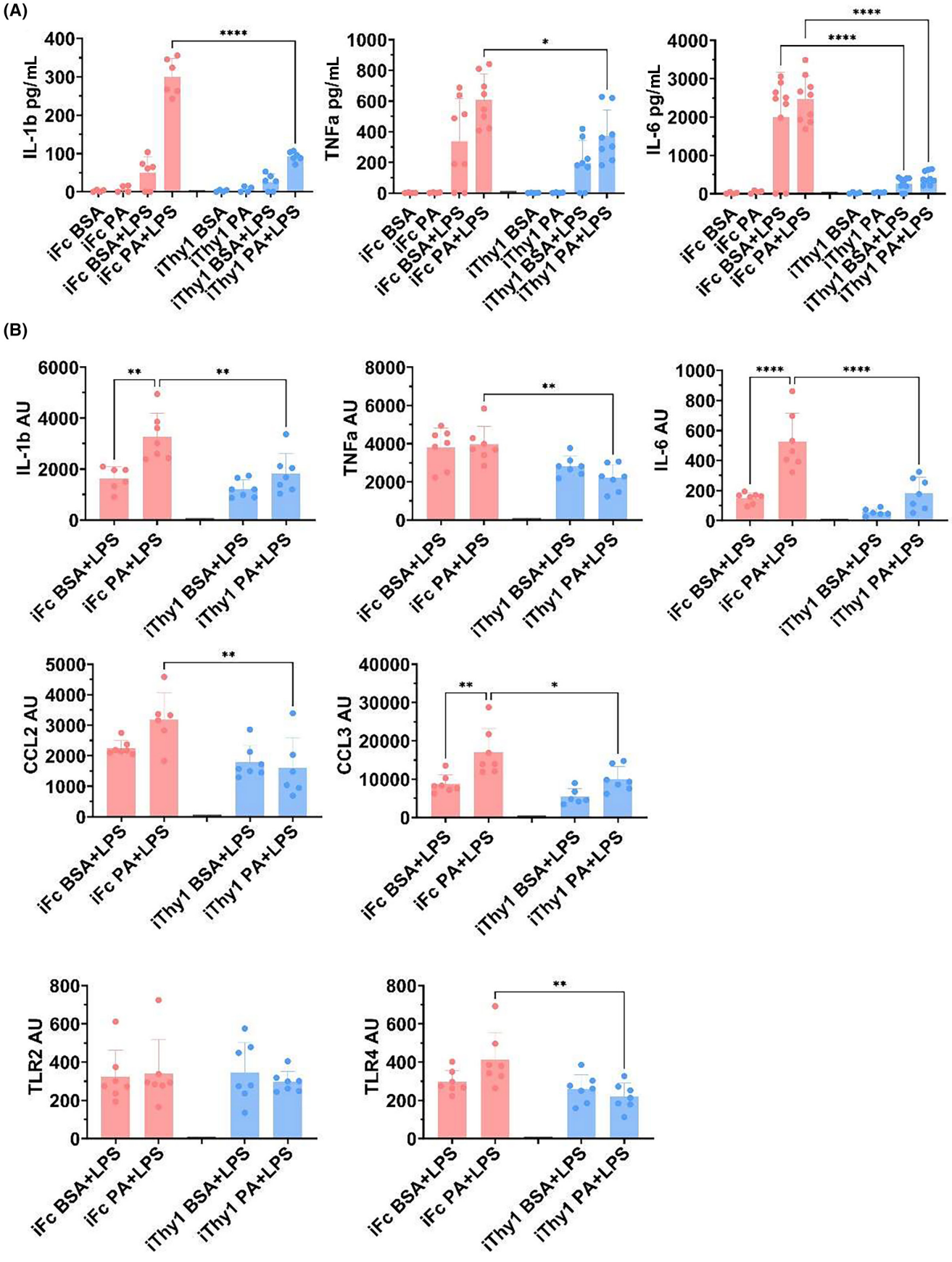

**FIGURE 5** Thy-1 prevents palmitic acid-mediated amplification of the LPS response in bone marrow cells. Bone marrow cells (BMCs) were isolated from WT mice and cultured on recombinant Thy-1-Fc (iThy1) or Fc-control protein (iFc). Cells were stimulated with LPS and 500 μM palmitic acid (PA) or bovine serum albumin (BSA). Cells without LPS were used as controls. (A) Detection of the indicated cytokines in the supernatant after 24 h by ELISA. (B) Gene expression of the indicated genes was detected by quantitative PCR. Each point represents the BMC from one mouse. The results are shown as the mean ± standard deviation. *p* Values were assessed by ANOVA. **p* < .05; ***p* < .01; *****p* < .0001.

**TABLE 1** Baseline characteristics of the study populations in cohorts 1 and 2.

| | Cohort 1 (*n* = 94) | Cohort 2 (*n* = 180) |
|---|---|---|
| Female sex (*N* (%)) | 48 (51%) | 104 (58%) |
| Diabetes (*N* (%)) | 60 (64%) | 180 (100%) |
| Age (years) | 62.3 [15.9] | 65.0 [17.0] |
| BMI (kg/m$^2$) | 28.9 [6.7] | 31.4 [9.7] |
| ALT (μkat/L) | .6 [.5] | .5 [.3] |
| AST (μkat/L) | .6 [.3] | .5 [.3] |
| sThy1 (pg/mL) | 3165.7 [1252.2] | 2729.8 [1318.7] |
| Fib4 score | 1.62 [1.00] | 1.5 [1.3] |
| FAST score | .137 [.139] | .3 [.4] |
| Controlled attenuation parameter (dB/m) | 297 [79] | 314 [73] |
| Liver stiffness measurement (kPa) | 4.8 [2.8] | 6.1 [5.6] |
| NAFLD fibrosis score | −1.01 [2.70] | .02 [1.80] |

*Note*: Baseline characteristics of the study populations in cohorts 1 and 2. The data are presented as numbers (%) or medians (interquartile ranges).

Abbreviations: AST, aspartate aminotransferase; ALT, alanine transaminase; BMI, body mass index; Fib4, fibrosis 4; FAST, FibroScan-AST; sThy1, soluble Thy-1.

positive correlation ($p = .049$) with sThy-1. In our second diabetic cohort, we confirmed the correlation of the serum sThy-1 concentration with the AST, NAFLD fibrosis score, Fib4 score, liver stiffness, and FAST score. To confirm the close association between sThy-1 and fibrosis risk, multiple linear regression analysis was carried out. Here, sThy-1 remained an independent and positive predictor of liver stiffness in both cohorts even after adjustment for age, sex, BMI, and diabetes status (Table 2).

Taken together, these findings suggest that the serum sThy-1 concentration is positively associated with the risk of liver fibrosis independent of age, sex, BMI, and diabetes status in human patients with MASLD.

## 4 | DISCUSSION

The increasing prevalence of SLD is a major challenge for healthcare systems worldwide. Approximately, one-third of affected patients

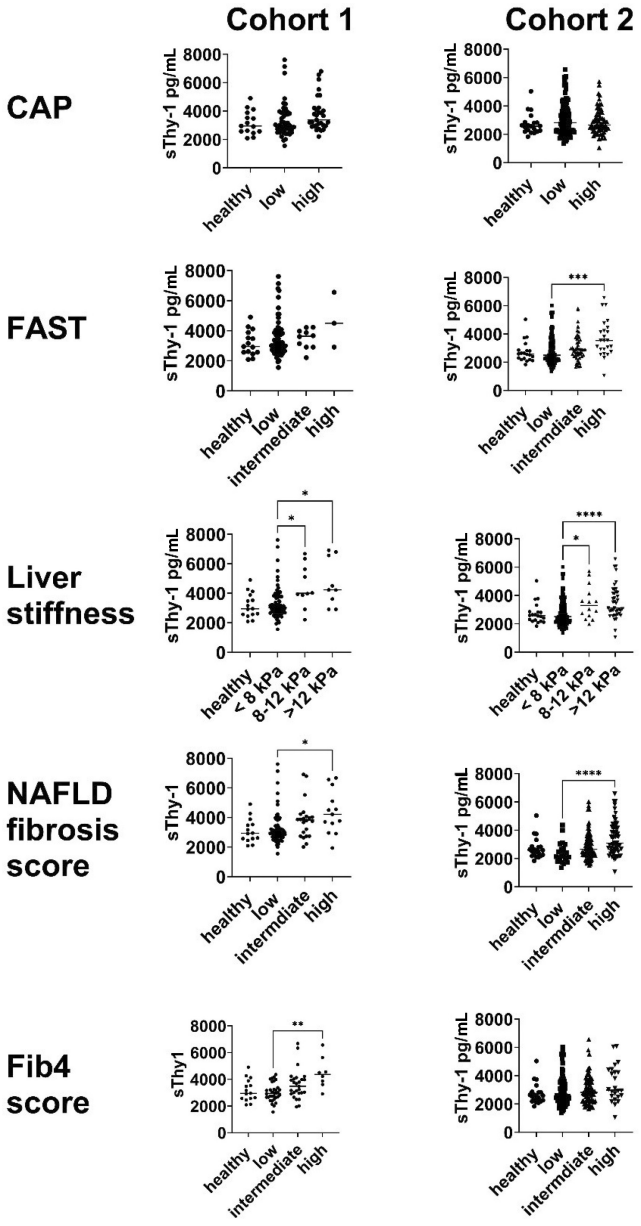


**FIGURE 6** Serum sThy-1 increases with fibrosis in patients with metabolically associated steatotic liver disease (MASLD). Soluble Thy-1 was detected in the serum of patients with MASLD and healthy controls in two different cohorts by ELISA. All patients in cohort 2 had a diagnosis of type 2 diabetes. Patients were stratified according to their steatosis, inflammation, and fibrosis grade as described in the Section 2. All the results are shown as the mean ± standard deviation. Overall *p* values were assessed by one-way ANOVA. **p* < .05; ***p* < .01; ****p* < .001, *****p* < .0001.

**TABLE 2** Univariate and multivariate correlation analyses of the association between the serum sThy-1 concentration and anthropometric and liver marker levels.

| | Univariat correlation analysis | | | | Multivariate linear regression analyses | | | |
|---|---|---|---|---|---|---|---|---|
| | Cohort 1 ($n=94$) | | Cohort 2 ($n=180$) | | Cohort 1 ($n=94$) | | Cohort 2 ($n=180$) | |
| | *r* | *p* | *r* | *p* | *β* | *p* | *β* | *p* |
| Age | **.226** | <.05 | .008 | n.s. | - | - | - | - |
| BMI | .194 | .06 | **.247** | <.01 | - | - | - | - |
| AST | **.281** | <.01 | **.154** | <.05 | - | - | - | - |
| CAP | **.218** | <.05 | −.052 | n.s. | | | | |
| FAST score | **.342** | <.01 | **.255** | <.01 | .205 | .06 | **.218** | <.01 |
| Liver stiffness measurement | **.445** | <.01 | **.369** | <.01 | **.307** | <.01 | **.356** | <.01 |
| NAFLD fibrosis score | **.339** | <.01 | **.36** | <.01 | | | | |
| Fib4 score | **.334** | <.01 | **.237** | <.01 | | | | |

*Note*: Univariate correlation analysis (left columns) and multivariate linear regression analysis (right columns) of sThy1 with anthropometric and liver markers in cohorts 1 and 2. The nonparametric Spearman's rank correlation method was used to assess univariate relationships between sThy1 and the indicated markers. Multivariate regression analyses were calculated for sThy1 (Lg, dependent variable) and the respective liver marker after adjustment for age, sex, BMI, and the presence of diabetes. Nonnormally distributed variables were assessed by the Shapiro–Wilk test and logarithmically transformed prior to multivariate testing. *r*- and *p* values, as well as standardized *β*-coefficients and *p* values, are given. Statistically significant correlations and associations ($p<.05$) are indicated in bold.

Abbreviations: AST, aspartate aminotransferase; BMI, body mass index; FAST, FibroScan-Aspartate aminotransferase.

will develop MASH syndrome, a major risk factor for further progression to more advanced liver fibrosis, cirrhosis, and cancer.[3,6,23] A better understanding of the detailed underlying pathogenic mechanisms of the transition from MASLD to MASH and ultimately to fibrosis is crucial for the design of new and efficient therapeutic interventions. In the present study, we demonstrated that Thy-1 attenuates the development of fatty liver disease and the expression of profibrotic genes in the liver of HFD-induced obese mice. The positive correlation between the serum sThy-1 concentration and liver fibrosis markers in patients with MASLD syndrome highlights the role of Thy-1 in the pathogenesis of SLD-associated liver fibrosis. Therefore, Thy-1 may represent an important target for further research focusing on the development and progression of SLD and could be a potential therapeutic target.

HFD-induced SLD mice with similar Western diet-related effects exhibit features similar to those of MASH in humans, but the pathological consequences are not severe.[49,50] In the present study, a HFD induced strong weight gain associated with a profound accumulation of TG in the liver. In addition, increased expression of profibrotic genes, such as collagen I/III and *Tgfβ1*, indicates the initiation of a profibrotic response.

Deletion of Thy-1 further strengthens liver steatosis upon HFD consumption, as determined by increased fat deposition. Serum TG and insulin are increased in Thy-1-KO mice, contributing to enhanced triglyceride accumulation in the liver. As shown earlier, loss of Thy-1 results in the accumulation of adipose tissue, which might explain the increase in the serum triglyceride and insulin levels in Thy-1-KO mice.[51]

Importantly, a lack of Thy-1 further increased the hepatic mRNA expression of profibrotic genes in the liver, indicating the protective role of Thy-1 in liver fibrosis development. Our data concerning the impact of Thy-1 on liver fibrosis are in accordance with those from other fibrosis mouse models. Thus, a lack of Thy-1 amplifies lung, heart and kidney fibrosis.[17,19,20,52] In the liver, Thy-1 deficiency exacerbates fibrosis in a mouse model of Mdr2 deficiency-induced cholestatic fibrosis.[19] Like in HFD-induced SLD mice, the expression of profibrotic genes was enhanced in Thy-1-deficient mice.[19] Thy-1 cells exhibit mainly periportal expression adjacent to the portal vein, arteries, and bile ducts, while Thy-1 expression is not detectable on HSCs.[23,53] Similarly, ECM deposition is detected in the periportal region together with the expansion of Thy-1-expressing mesenchymal cells during cholestatic liver injury.[54]

Taken together, these data indicate an antifibrotic role of Thy-1 in organ fibrosis. The effects of Thy-1 on liver fibrosis might be direct through its action on ECM-producing cells or indirect through its action on inflammatory cells. Indeed, Thy-1 restricts the profibrotic action of NPC. Several mechanisms for direct Thy-1-mediated control of fibrosis have already been described. Thy-1 supports apoptosis in lung and skin fibroblasts via Fas-, Bcl-, and caspase-dependent pathways.[55] Consequently, Thy-1 knockout mice exhibit enhanced fibroblast proliferation, reduced apoptosis and a decreased Fas ligand.[22,56] Inhibition of apoptosis in Thy-1-deficient mice leads to the persistence of myofibroblasts during the resolution phase of bleomycin-induced lung fibrosis.[55] Consistently, Thy-1 inhibits proliferation and supports apoptosis in NPC cells. Moreover, we showed that Thy-1 inhibits the expression of profibrotic genes in NPC.

Moreover, the interaction of Thy-1 *in cis* with integrins and growth factor receptors regulates the fibrogenic actions of fibroblasts. Thy-1 inhibits fibroblast contraction-induced latent TGFβ1 activation and TGFβ1-dependent lung myofibroblast differentiation

via interaction with integrin αvβ5.[57] Moreover, Thy-1-negative, but not Thy-1-positive, rat lung fibroblasts respond to profibrotic cytokines via the activation of latent Tgfβ1 and exhibit greater myofibroblast gene expression and greater collagen contraction than Thy-1-positive cells.[58,59] Koyama et al. demonstrated that Thy-1 inhibits TGFβ-RI signalling.[60] TGFβ1 stimulation facilitates the binding of mesothelin (Msln) to Thy-1, thereby promoting the dissociation of Thy-1 from TGFβ-RI and enabling TGFβ1/TGFβ-RI signalling in lung and portal fibroblasts. Deletion of *Msln* in activated portal fibroblasts results in strong overexpression of Thy-1, which in turn binds to TGFβ-RI and prevents TGFβ1 signalling.[19,60] Deletion of Thy-1 strengthens fibrosis, while a lack of *Msln* reduces fibrosis in this model. We propose that a similar mechanism might act in our mouse model of HFD-induced SLD. Several reports indicate a positive feedback loop of TGFβ1. Zhang et al. identified TGFβ1 as a TGFβ1-target gene.[61] Xu et al demonstrate that TGFβ1 stimulates TET3 expression in HSCs, which in turn supports TGFβ1expression.[62] We hypothesize that Thy-1-mediated inhibition of TGFβ1 signalling interrupts the viscous cycle of uncontrolled TGFβ1-mediated matrix production in HFD-induced SLD. Taken together, these findings indicate that Thy-1-deficient mice are more susceptible to fibrosis, suggesting that Thy-1 is critical for the control of fibroblast activation and has an antifibrotic function.

Macrophages are the first cells to respond to liver injury-inducing inflammation. Importantly, uncontrolled, persistent inflammation drives liver fibrosis, ultimately leading to liver cirrhosis.[10] In the present study, we demonstrated that loss of Thy-1 results in an increase in the number of inflammatory cells within the liver. In addition, the expression of proinflammatory cytokines such as IL-1β and TNFα is increased. In vitro studies of proinflammatory activated bone marrow cells on recombinant Thy-1 prove the inhibitory role of Thy-1. Thus, Thy-1-mediated inhibition of macrophage activation might indirectly contribute to the antifibrotic effect of Thy-1. Importantly, Thy-1 inhibits PA-mediated amplification of the inflammatory response. It has been hypothesized that saturated free fatty acids such as PAs directly activate TLR4, classically inducing the proinflammatory activation of macrophages.[63] Lancaster et al. demonstrated that saturated free fatty acids are not TLR4 agonists but provide a second hit of activation, strengthening the LPS response.[64] The inhibition of TLR4 expression by Thy-1 upon LPS stimulation in the presence of high PA might explain the anti-inflammatory effect of Thy-1. However, the mechanisms underlying the anti-inflammatory action of Thy-1 in the presence of FFA are still unclear.

In addition to its membrane form, a soluble form of Thy-1 has been detected in the serum; in the urine; and in the wound, synovial, and cerebrospinal fluid.[15,65,66] In the present study, we showed that the serum sThy-1 concentration was positively correlated with the risk of advanced liver fibrosis, as assessed by liver stiffness, the Fib4 score, and the NAFLD fibrosis score. Consistent with our data, gene expression analysis of liver biopsies from 206 MASLD patients revealed that the expression of Thy-1 increases with the progression of MASLD, especially with the development of fibrosis.[67] In contrast, circulating sThy-1 levels were not significantly associated with the hepatic steatosis grade. The positive association between sThy-1 and the FAST score suggested that inflammation has an impact on sThy-1. However, the FAST score is determined by the combination of liver stiffness, CAP and AST levels. Thus, we cannot exclude the possibility that this association is related to the strong correlation of the serum sThy-1 concentration with fibrosis stage. There are no histological data available in our cohorts to validate the relationship between the serum sThy-1 concentration and tissue inflammation; therefore, further research should include a histological reference standard. Furthermore, in accordance with our data, increased sThy-1 has been detected in patients with systemic sclerosis, as well as in patients with diabetic kidney disease, which is associated with renal fibrosis.[66,68,69]

The positive correlation between the serum Thy-1 concentration and liver fibrosis in patients with MASLD syndrome appears to be counterintuitive because of the protective effect of Thy-1 on the development of liver fibrosis in our mouse model of SLD. Interestingly, in this context, for the adipocytokine FGF21, an apparently similar paradox expression pattern has been described.[70,71] Thus, the metabolic beneficial cytokine FGF21 is increased in metabolic disease states, including patients with MASLD, most likely through FGF21 resistance.[70,71] However, whether Thy-1 signalling is affected in SLD is still an open question. In addition, more than 150 types of proteins are expected to be anchored to the plasma membrane via a GPI site. GPI-specific phospholipase D (GPI-PLD) is a secreted protein that specifically hydrolyses the glycan-phosphatidylinositol linkages of GPI anchors.[72] Since Thy-1 is a GPI-anchored protein, it can be cleaved by GPI-PLD.[14] GPI-PLD is highly expressed in the liver. Moreover, hepatic mRNA levels and circulating concentrations of GPI-specific PLD are significantly enhanced in diabetic mice. Since Thy-1 mRNA levels are not changed in obese and *db/db* mice, alterations in GPI-PLD expression or activity might contribute to enhanced sThy-1 in the SLD. In addition, increased soluble Thy-1 levels might reflect a counterregulatory mechanism.

In conclusion, a lack of Thy-1 increases susceptibility to the expression of profibrotic genes in mice and facilitates the proinflammatory activation of macrophages. Moreover, circulating sThy-1 is significantly associated with the risk of advanced fibrosis in patients with MASLD. These data indicate that Thy-1 may function as an important antifibrotic factor in liver fibrosis.

## AUTHOR CONTRIBUTIONS

AS, TE, VB, and TK designed the study. AS performed the experiments, evaluated and analysed the data and wrote the manuscript. UA contributed to the analysis and interpretation of the data. VB, TK, and JW performed patient characterization and collected samples. LB, DLD, and JA performed the statistical analysis of the RNA-Seq data. CK provided experience in the isolation of liver cells. All the authors discussed the data and study design and read and edited the manuscript.

## ACKNOWLEDGEMENTS

We thank Danny Gutknecht and Ulrike Lössner for excellent technical assistance. Open Access funding enabled and organized by Projekt DEAL.

## FUNDING INFORMATION

We acknowledge the support of the University Leipzig within the program Open Access Publishing. This work was supported by a grant from DFG (SA 863/9-1) and by the DFG SFB 1052 project B10. The patient cohorts were recruited from clinical research projects of the IFB AdiposityDiseases Leipzig, Germany (supported by the Federal Ministry of Education and Research [BMBF], Germany; FKZ: 01EO1001). ThE was supported by a Novo Nordisk postdoctoral fellowship run in partnership with Karolinska Institutet, Stockholm, Sweden; a Karolinska Institute Research Foundation grant; the Stiftelsen Stig och Gunborg Westman; the Swedish Kidney Foundation (Njurfonden); the German Diabetes Association (DDG); and the Team Award Nephrology+2023 by Otsuka Pharma. ThE was further funded through the EFSD Mentorship Programme supported by AstraZeneca. CK was supported by the BMBF-funded project LiSyM-Cancer [031L0258E; 031L0256C].

## CONFLICT OF INTEREST STATEMENT

The authors declare that no conflicts of interest exist.

## ETHICS STATEMENT

The studies were approved by the local ethical committee (Leipzig University, registration numbers 283-11-22082011, 419-12-17122012, 035/17-ek). Informed written consent was obtained from all participants, and the studies were performed in accordance with the guidelines for good clinical practice and the ethical guidelines of the Helsinki Declaration.

## ORCID

*Valentin Blank* https://orcid.org/0000-0003-0457-4135
*Thomas Karlas* https://orcid.org/0000-0002-8109-8526
*Johannes Wiegand* https://orcid.org/0000-0001-9233-4064
*Christiane Körner* https://orcid.org/0000-0001-8753-8441
*Anja Saalbach* https://orcid.org/0000-0002-1084-3875

## REFERENCES

1. Arab JP, Arrese M, Trauner M. Recent insights into the pathogenesis of nonalcoholic fatty liver disease. *Annu Rev Pathol Mech Dis*. 2018;13:321-350.
2. Francque SM, Marchesini G, Kautz A, et al. Non-alcoholic fatty liver disease: a patient guideline. *JHEP Reports*. 2021;3:100322.
3. Tacke F, Canbay A, Bantel H, et al. Updated S2k clinical practice guideline on non-alcoholic fatty liver disease (NAFLD) issued by the German Society of Gastroenterology, digestive and metabolic diseases (DGVS) – April 2022 – AWMF registration No.: 021–025. *Z Gastroenterol*. 2022;60:e733-e801.
4. Ebert T, Linder N, Schaudinn A, et al. Association of fetuin B with markers of liver fibrosis in nonalcoholic fatty liver disease. *Endocrine*. 2017;58:246-252.
5. Ray G. Management of liver diseases: current perspectives. *World J Gastroenterol*. 2022;28:5818-5826.
6. Quek J, Chan KE, Wong ZY, et al. Global prevalence of non-alcoholic fatty liver disease and non-alcoholic steatohepatitis in the overweight and obese population: a systematic review and meta-analysis. *Lancet Gastroenterol Hepatol*. 2023;8:20-30.
7. Younossi ZM, Koenig AB, Abdelatif D, Fazel Y, Henry L, Wymer M. Global epidemiology of nonalcoholic fatty liver disease-meta-analytic assessment of prevalence, incidence, and outcomes. *Hepatology*. 2016;64:73-84.
8. Van Herck M, Vonghia L, Francque S. Animal models of nonalcoholic fatty liver disease—a Starter's guide. *Nutrients*. 2017;9:1072.
9. Chen Z, Tian R, She Z, Cai J, Li H. Role of oxidative stress in the pathogenesis of nonalcoholic fatty liver disease. *Free Radic Biol Med*. 2020;152:116-141.
10. Wen Y, Lambrecht J, Ju C, Tacke F. Hepatic macrophages in liver homeostasis and diseases-diversity, plasticity and therapeutic opportunities. *Cell Mol Immunol*. 2021;18:45-56.
11. Mederacke I, Hsu CC, Troeger JS, et al. Fate tracing reveals hepatic stellate cells as dominant contributors to liver fibrosis independent of its aetiology. *Nat Commun*. 2013;4:2823.
12. Zheng J, Wu H, Zhang Z, Yao S. Dynamic co-expression modular network analysis in nonalcoholic fatty liver disease. *Hereditas*. 2021;158:31. doi:10.1186/s41065-021-00196-8
13. Saalbach A, Anderegg U. Thy-1: more than a marker for mesenchymal stromal cells. *FASEB J*. 2019;33:6689-6696.
14. Saalbach A, Kraft R, Herrmann K, Haustein UF, Anderegg U. The monoclonal antibody AS02 recognizes a protein on human fibroblasts being highly homologous to Thy-1. *Arch Dermatol Res*. 1998;290:360-366.
15. Saalbach A, Wetzig T, Haustein UF, Anderegg U. Detection of human soluble Thy-1 in serum by ELISA. *Cell Tissue Res*. 1999;298:307-315.
16. Hu P, Leyton L, Hagood JS, Barker TH. Thy-1-integrin interactions in cis and trans mediate distinctive signaling. *Front Cell Dev Biol*. 2022;10:1-20.
17. Li Y, Song D, Mao L, Abraham DM, Bursac N. Lack of Thy1 defines a pathogenic fraction of cardiac fibroblasts in heart failure. *Biomaterials*. 2020;236:119824.
18. Acharya P, Chouhan K, Weiskirchen S, Weiskirchen R. Cellular mechanisms of liver fibrosis. *Front Pharmacol*. 2021;12:671640.
19. Nishio T, Koyama Y, Liu X, et al. Immunotherapy-based targeting of MSLN + activated portal fibroblasts is a strategy for treatment of cholestatic liver fibrosis. *Proc Natl Acad Sci*. 2021;118:118.
20. Hagood JS, Prabhakaran P, Kumbla P, et al. Loss of fibroblast Thy-1 expression correlates with lung Fibrogenesis. *Am J Pathol*. 2005;167:365-379.
21. Marangoni RG, Datta P, Paine A, et al. Thy-1 plays a pathogenic role and is a potential biomarker for skin fibrosis in scleroderma. *JCI Insight*. 2022;7:e149426.
22. Schmidt M, Gutknecht D, Simon JC, et al. Controlling the balance of fibroblast proliferation and differentiation: impact of thy-1. *J Invest Dermatol*. 2015;135:1893-1902.
23. Dudas J, Mansuroglu T, Batusic D, Ramadori G. Thy-1 is expressed in myofibroblasts but not found in hepatic stellate cells following liver injury. *Histochem Cell Biol*. 2009;131:115-127.
24. Chalasani N, Younossi Z, Lavine JE, et al. The diagnosis and Management of non-alcoholic Fatty Liver Disease: practice guideline by the American Association for the Study of Liver Diseases, American College of Gastroenterology, and the American Gastroenterological Association. *Am J Gastroenterol*. 2012;107:811-826.
25. Rinella ME, Lazarus JV, Ratziu V, et al. A multisociety Delphi consensus statement on new fatty liver disease nomenclature. *J Hepatol*. 2023;79:1542-1556. doi:10.1016/j.jhep.2023.06.003

26. Karlas T, Berger J, Garnov N, et al. Estimating steatosis and fibrosis: comparison of acoustic structure quantification with established techniques. *World J Gastroenterol*. 2015;21:4894-4902.
27. Karlas T, Petroff D, Garnov N, et al. Non-invasive assessment of hepatic steatosis in patients with NAFLD using controlled attenuation parameter and 1H-MR spectroscopy. *PLoS One*. 2014;9:e91987.
28. Blank V, Petroff D, Beer S, et al. Current NAFLD guidelines for risk stratification in diabetic patients have poor diagnostic discrimination. *Sci Rep*. 2020;10:18345.
29. Săftoiu A, Gilja OH, Sidhu PS, et al. The EFSUMB guidelines and recommendations for the clinical practice of Elastography in non-hepatic applications: update 2018. *Ultraschall Med*. 2019;40:425-453.
30. Eddowes PJ, Sasso M, Allison M, et al. Accuracy of FibroScan controlled attenuation parameter and liver stiffness measurement in assessing steatosis and fibrosis in patients with nonalcoholic fatty liver disease. *Gastroenterology*. 2019;156:1717-1730.
31. Ravaioli F, Dajti E, Mantovani A, Newsome PN, Targher G, Colecchia A. Diagnostic accuracy of FibroScan-AST (FAST) score for the non-invasive identification of patients with fibrotic non-alcoholic steatohepatitis: a systematic review and meta-analysis. *Gut*. 2023;72:1399-1409.
32. Newsome PN, Sasso M, Deeks JJ, et al. FibroScan-AST (FAST) score for the non-invasive identification of patients with non-alcoholic steatohepatitis with significant activity and fibrosis: a prospective derivation and global validation study. *Lancet Gastroenterol Hepatol*. 2020;5:362-373.
33. Sterling RK, Lissen E, Clumeck N, et al. Development of a simple noninvasive index to predict significant fibrosis in patients with HIV/HCV coinfection. *Hepatology*. 2006;43:1317-1325.
34. McPherson S, Hardy T, Dufour J-F, et al. Age as a confounding factor for the accurate non-invasive diagnosis of advanced NAFLD fibrosis. *Am J Gastroenterol*. 2017;112:740-751.
35. Nosten-Bertrand M, Errington ML, Murphy KP, et al. Normal spatial learning despite regional inhibition of LTP in mice lacking Thy-1. *Nature*. 1996;379:826-829.
36. Kaiser F, Morawski M, Krohn K, et al. Adhesion GPCR GPR56 expression profiling in human tissues. *Cells*. 2021;10:3557.
37. Chen S, Zhou Y, Chen Y, Gu J. Fastp: an ultra-fast all-in-one FASTQ preprocessor. *Bioinformatics*. 2018;34:i884-i890.
38. Kim D, Langmead B, Salzberg SL. HISAT: a fast spliced aligner with low memory requirements. *Nat Methods*. 2015;12:357-360.
39. Pertea M, Kim D, Pertea GM, Leek JT, Salzberg SL. Transcript-level expression analysis of RNA-seq experiments with HISAT, StringTie and Ballgown. *Nat Protoc*. 2016;11:1650-1667.
40. Love MI, Huber W, Anders S. Moderated estimation of fold change and dispersion for RNA-seq data with DESeq2. *Genome Biol*. 2014;15:550.
41. Yu G, Wang L-G, Han Y, He Q-Y. clusterProfiler: an R package for comparing biological themes among gene clusters. *Omi A J Integr Biol*. 2012;16:284-287.
42. Draghici S, Khatri P, Tarca AL, et al. A systems biology approach for pathway level analysis. *Genome Res*. 2007;17:1537-1545.
43. Ashburner M, Ball CA, Blake JA, et al. Gene ontology: tool for the unification of biology. *Nat Genet*. 2000;25:25-29.
44. Carbon S, Douglass E, Good BM, et al. The gene ontology resource: enriching a GOld mine. *Nucleic Acids Res*. 2021;49:D325-D334.
45. Wickham H, Averick M, Bryan J, et al. Welcome to the Tidyverse. *J Open Source Softw*. 2019;4:1686.
46. Wickham H. Reshaping data with the reshape package. *J Stat Softw*. 2007;21:1-20.
47. Stelzner K, Herbert D, Popkova Y, et al. Free fatty acids sensitize dendritic cells to amplify TH1/TH17-immune responses. *Eur J Immunol*. 2016;46:2043-2053.
48. Medina-Montano C, Cacicedo ML, Svensson M, et al. Enrichment methods for murine liver non-parenchymal cells differentially affect their Immunophenotype and responsiveness towards stimulation. *Int J Mol Sci*. 2022;23:6543.
49. Zhong F, Zhou X, Xu J, Gao L. Rodent models of nonalcoholic fatty liver disease. *Digestion*. 2020;101:522-535.
50. Preguiça I, Alves A, Nunes S, et al. Diet-induced rodent models of obesity-related metabolic disorders—a guide to a translational perspective. *Obes Rev*. 2020;21:e13081.
51. Picke A-K, Campbell GM, Blüher M, et al. Thy-1 (CD90) promotes bone formation and protects against obesity. *Sci Transl Med*. 2018;10:eaao6806.
52. Chen L, Tang R-Z, Ruan J, Zhu X-B, Yang Y. Up-regulation of THY1 attenuates interstitial pulmonary fibrosis and promotes lung fibroblast apoptosis during acute interstitial pneumonia by blockade of the WNT signaling pathway. *Cell Cycle*. 2019;18:670-681.
53. Dudas J, Mansuroglu T, Batusic D, Saile B, Ramadori G. Thy-1 is an in vivo and in vitro marker of liver myofibroblasts. *Cell Tissue Res*. 2007;329:503-514.
54. Katsumata LW, Miyajima A, Itoh T. Portal fibroblasts marked by the surface antigen Thy1 contribute to fibrosis in mouse models of cholestatic liver injury. *Hepatol Commun*. 2017;1:198-214.
55. Liu X, Wong SS, Taype CA, et al. Thy-1 interaction with Fas in lipid rafts regulates fibroblast apoptosis and lung injury resolution. *Lab Investig*. 2017;97:256-267.
56. Schmidt M, Gutknecht D, Anastassiadis K, Eckes B, Anderegg U, Saalbach A. Thy-1/beta3 integrin interaction-induced apoptosis of dermal fibroblasts is mediated by up-regulation of FasL expression. *JInvest Dermatol*. 2016;136:526-529.
57. Zhou Y, Hagood JS, Lu B, Merryman WD, Murphy-Ullrich JE. Thy-1-integrin alphav beta5 interactions inhibit lung fibroblast contraction-induced latent transforming growth factor-beta1 activation and myofibroblast differentiation. *JBiolChem*. 2010;285:22382-22393.
58. Sanders YY, Kumbla P, Hagood JS. Enhanced Myofibroblastic differentiation and survival in Thy-1(–) lung fibroblasts. *Am J Respir Cell Mol Biol*. 2007;36:226-235.
59. Zhou Y, Hagood JS, Murphy-Ullrich JE. Thy-1 expression regulates the ability of rat lung fibroblasts to activate transforming growth factor-beta in response to fibrogenic stimuli. *AmJPathol*. 2004;165:659-669.
60. Koyama Y, Wang P, Liang S, et al. Mesothelin/mucin 16 signaling in activated portal fibroblasts regulates cholestatic liver fibrosis. *J Clin Invest*. 2017;127:1254-1270.
61. Zhang Y, Handley D, Kaplan T, et al. High throughput determination of TGFβ1/SMAD3 targets in A549 lung epithelial cells. *PLoS One*. 2011;6:e20319.
62. Xu Y, Sun X, Zhang R, et al. A positive feedback loop of TET3 and TGF-β1 promotes liver fibrosis. *Cell Rep*. 2020;30:1310-1318.e5.
63. Rogero M, Calder P. Obesity, inflammation, toll-like receptor 4 and fatty acids. *Nutrients*. 2018;10:432.
64. Lancaster GI, Langley KG, Berglund NA, et al. Evidence that TLR4 is not a receptor for saturated fatty acids but mediates lipid-induced inflammation by reprogramming macrophage metabolism. *Cell Metab*. 2018;27:1096-1110.
65. Almqvist P, Carlsson SR. Characterization of a hydrophilic form of Thy-1 purified from human cerebrospinal fluid. *J Biol Chem*. 1988;263:12709-12715.
66. Kollert F, Christoph S, Probst C, et al. Soluble CD90 as a potential marker of pulmonary involvement in systemic sclerosis. *Arthritis Care Res*. 2013;65:281-287.
67. Gao R, Wang J, He X, et al. Comprehensive analysis of endoplasmic reticulum-related and secretome gene expression profiles in the progression of non-alcoholic fatty liver disease. *Front Endocrinol (Lausanne)*. 2022;13:1-14.
68. Wu L, Chang D-Y, Zhang L-X, Chen M, Zhao M-H. Urinary soluble CD90 predicts renal prognosis in patients with diabetic kidney disease. *Ann Transl Med*. 2021;9:282.

69. Saalbach A, Anderegg U, Wendt R, et al. Antifibrotic soluble Thy-1 correlates with renal dysfunction in chronic kidney disease. *Int J Mol Sci*. 2023;24:1896.
70. Tucker B, Li H, Long X, Rye K-A, Ong KL. Fibroblast growth factor 21 in non-alcoholic fatty liver disease. *Metabolism*. 2019;101:153994.
71. Spann RA, Morrison CD, den Hartigh LJ. The nuanced metabolic functions of endogenous FGF21 depend on the nature of the stimulus, tissue source, and experimental model. *Front Endocrinol (Lausanne)*. 2022;12:802541.
72. Masuda S, Fujishima Y, Maeda N, et al. Impact of glycosylphosphatidylinositol-specific phospholipase D on hepatic diacylglycerol accumulation, steatosis, and insulin resistance in diet-induced obesity. *Am J Physiol Metab*. 2019;316:E239-E250.

## SUPPORTING INFORMATION

Additional supporting information can be found online in the Supporting Information section at the end of this article.

**How to cite this article:** Blank V, Karlas T, Anderegg U, et al. Thy-1 restricts steatosis and liver fibrosis in steatotic liver disease. *Liver Int*. 2024;44:2075-2090. doi:10.1111/liv.15956